Measurement of glass transition temperature, residual heat of reaction and mixing ratio of epoxy resins using near infrared spectroscopy: a preliminary study

Lars Plejdrup Houmøller[a] and Peter Clemen Laursen[b]

[a]*Aalborg University Esbjerg, Niels Bohrs Vej 8, 6700 Esbjerg, Denmark. E-mail: lph@aue.auc.dk*

[b]*Cheminova A/S, PO Box 9, 7620 Lemvig, Denmark. E-mail: pcl@cheminova.dk*

As a measure of the degree of curing of epoxy resins, the glass transition temperature, T_g, and the residual heat of reaction, ΔH_r, are often used. In this study, near infrared spectroscopy and multivariate calibration [partial least squares regression (PLSR)] have been used to monitor the two variables, using differential scanning calorimetry (DSC) as the reference method. The epoxy under study was a commercial system consisting of the resin, trimethylolpropanetriglycidylether, and the hardener, 3-aminomethyl-3,5,5,-trimethylcyclohexylamine. Using samples cured under different conditions, calibrations resulted in root mean square errors of cross-validation (*RMSECV*) of 18 Jg^{-1} for ΔH_r (range for ΔH_r: 6.1–231.3 Jg^{-1}) and 7.2°C for T_g (range for T_g: 41.5–98.8°C). Also, a PLSR model for mixing ratio of hardener and resin was obtained, resulting in a *RMSECV* of 0.0040 (range for mixing ratio: 0.180–0.380).

Keywords: NIR spectroscopy, epoxy resin, glass transition temperature, residual heat of reaction, mixing ratio

Introduction

Near infrared spectroscopy has been used in several studies[1–35] to investigate the curing characteristics of epoxy resins (for examples of review articles on NIR spectroscopy and polymers, see References 36–38). At specific wavelengths, the appearance or disappearance of functional groups can be followed and reaction kinetics derived. For practical and industrial purposes, however, quantitative meaures of the degree of curing are needed. Often, differential scanning calorimetry (DSC) is used for this purpose, resulting in two parameters: the glass transition temperature, T_g, and the residual heat of reaction, ΔH_r. The glass transition temperature is defined as the point at which the polymer changes from a glassy to a rubbery state and ΔH_r is a measure of the number of unreacted groups in the polymer.

Details of DSC, which can be found in the literature[39-41] on this subject, will not be outlined here.

Epoxy resins find many applications in industry; this paper concerns coatings on wings for windmills. At a major windmill factory, an outer layer of epoxy (called "gelcoat") is applied to the wings as a protection against ultraviolet radiation. As part of a comprehensive study of the curing characteristics of the gelcoat, it was necessary to obtain a measure of

the degree of curing. As an alternative to the laborious and time-consuming DSC analysis, NIR spectroscopy was investigated as a method of quantitative analysis of the gelcoat samples.

Apart from the curing characteristics, also the mixing ratio of the hardener and resin is a very important parameter, which should be kept close to the specification. To check the mixing ratio in the cured product, NIR spectra of samples with varying mixing ratios were obtained.

The study consisted of three parts:

(1) monitoring of the curing as a function of time at three different (fixed) temperatures
(2) monitoring of the curing as a function of time at the last temperature of two different temperature programs I and II (consisting of two and three temperatures respectively)
(3) performing a quantitative calibration for mixing ratio, using the same temperature program for the calibration samples.

In this paper, the part of the study concerning the use of NIR will be presented.

Experimental

The gelcoat (supplied by SP Systems, UK) consists of a resin, trimethylolpropanetriglycidylether, and a hardener, 3-aminomethyl-3,5,5,-trimethyl-cyclohexylamine. The specified mixing ratio by weight is hardener : resin = 28 : 100.

In Part 1 of the study, the gelcoat was applied to glass plates and allowed to cure at three different temperatures, and for each temperature diffuse reflectance NIR spectra were obtained at four times (different for the three temperatures).

For Parts 2 and 3, the gelcoat was applied to a mould and heated at a temperature, T_1, for a time, t_1, after which two layers of epoxy "prepreg" (SP Systems, UK) were applied to the gelcoat. The prepreg constitutes the inner part of the windmill wing; therefore these experiments resemble the actual process of fabrication.

In Part 2, for temperature Program I, the prepreg and gelcoat was heated at T_2 for three different times, t_2, after which the samples were removed from the mould and diffuse reflectance NIR spectra of the gelcoat were acquired.

For temperature Program II, the treatment consisted of heating at T_2 for a fixed time, t_2, and then heating at T_3 for seven different times, t_3.

In Part 3, the mixing ratio of hardener and resin was varied from 18 : 100 to 38 : 100 (13 samples) and cured using the same temperature program.

Temperatures, times, mixing ratios, glass transition temperatures and residual heats of reaction are shown in Tables 1(a) and 1(b).

NIR spectra were acquired on a Bomem MB160 FT-NIR spectrometer (ABB Bomem) equipped with the Powder Sampl*ir* accessory for diffuse reflectance. The sample was placed horizontally on the window (diameter 12 mm) without any pre-treatment. The wavenumber range was 3800–12000 cm^{-1} (wavelength range 830–2630 nm) and the distance between data points was 8 cm^{-1} (1065 data points).

For background spectrum, an average of 200 scans on a "Spectralon" (Labsphere) was used and for the samples, an average of 100 scans was used. The effect of the spectral noise on the calibration models has not been investigated and a lower number of scans might be sufficient.

DSC analysis was carried out in triplicate for Parts 1 and 2 (for Part 3 only one DSC analysis was performed on each sample) on a Mettler DSC 20 with TC11 Processor. The initial temperature was 25°C and the heating rate was 10°C min^{-1}. The mean values of ΔH_r and T_g were used for calibration.

The software used for data analysis and calibration was MATLAB R12 (The MathWorks) and The Unscrambler 7.6 (CAMO ASA).

Results and discussion

To illustrate the determination of T_g and ΔH_r, an example from a DSC experiment is shown in Figure 1. Two horizontal lines, before and after the negatively sloping part of the curve, are constructed and the onset and endpoint are defined as the points of intersection of these lines and a line through the inflection point. T_g is then defined as the temperature of the midpoint between the onset and endpoint. ΔH_r is the hatched area of the positive peak.

The raw spectra for Parts 1–3 (35 samples) and multiplicative signal corrected[42] (MSC) spectra are shown in Figure 2(a) and (b). The wavenumber

Table 1(a). Temperatures, times, glass transition temperatures and residual heats of reaction for Parts 1 and 2 of the curing experiments.

Part	Temp. program	T_1 (°C)	t_1 (min)	T_2 (°C)	t_2 (min)	T_3 (°C)	t_3 (min^{-1})	T_g[a] (°C)	ΔH_r[a] (J g^{-1})
1		20	60						231.3
			180						167.0
			290						138.1
			3010					44.8	41.5
		50	40						127.0
			120					48.4	34.0
			240					58.5	22.9
			1440					71.0	10.0
		120	20					73.8	
			60					84.8	
			180					92.7	
			300					94.7[b]	
2	I	50	38	90	10			64.5	15.2
					20			68.6	11.6
					30			70.9	6.1
	II	50	38	90	30	120	10	82.0	
							20	86.1	
							40	86.1	
							60	94.1	
							80	90.3	
							180	92.5	
							300	88.2	

mixing ratio hardener : resin = 28 : 100
[a]mean values of triplicates
[b]sample detected as outlier and removed from the calibration model for T_g

Table 1(b). Mixing ratios and glass transition temperatures for Part 3 of the curing experiments.

Part 3	Temp. program: 20–90°C in 25 min, 30 min at 90°C, 90-120°C in 20 min, 60 min at 120°C												
h : r[c]	0.18	0.20	0.22	0.24	0.26	0.27	0.28[d]	0.29	0.30	0.32[d]	0.34	0.36	0.38
T_g (°C)	82.5[b]	98.8[b]	53.9	69.6	78.2	78.3	79.0	76.0	73.3	75.8	66.9	65.3	58.0

[b]samples detected as outliers and removed from the calibration model for T_g
[c]mixing ratio hardener : resin
[d]samples detected as outliers and removed from the calibration model for mixing ratio

range above approx. 9000 cm^{-1} showed no spectral features and did not contribute to the calibration models and, therefore, the range 9003–12000 cm^{-1} was omitted from the plots and the calibrations. The explanation of the negative absorbances at some wavenumbers is that different gain settings were used for the background and samples, respectively. As is often seen in reflectance spectra, the raw spectra show scatter effects, which can be removed using the pre-treatment MSC. This usually improves the calibration models, which was also shown to be the case in this study.

To illustrate the spectral changes during curing, the four spectra cured at 20°C in Part 1 were transformed using the standard normal variate (SNV) and detrending,[43] which is an often used pre-treatment to visualise spectral differences. The spectrum for the time t_1 was subtracted from each spectrum to give SNV detrended difference spectra (Figure 3).

Also, the spectral effect of changing the mixing ratio of hardener and resin can be shown using SNV and detrended difference spectra (Figure 4).

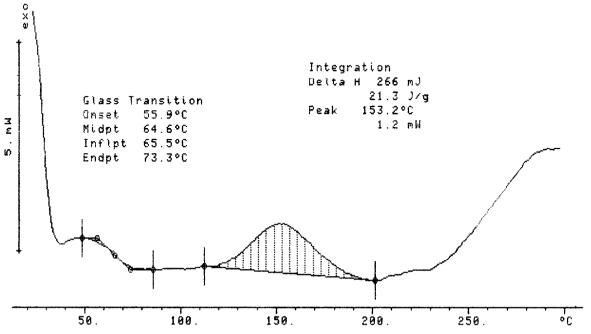Assignments of some of the bands in Figures 3 and 4 are given in Table 2.

Figure 1. DSC analysis of a sample from Part 1 of the curing experiments. Sample mass = 12.5 mg. T_g = 64.6°C, ΔH_r = 21.3 Jg^{-1}.
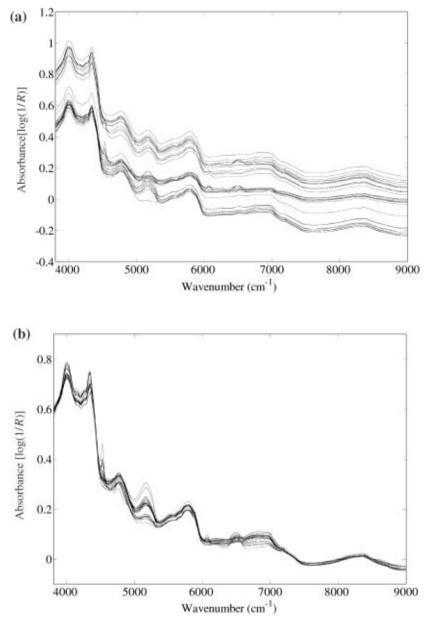
Figure 2. (a) Raw spectra of all (35) samples. (b) Spectra of all (35) samples after MSC.

As expected, Figure 3 shows the disappearance of epoxy and amine functional groups and the appearance of hydroxyl groups, as a function of reaction time. Figure 4 shows the increasing amount of primary amine from the hardener compared to the epoxy group from the resin.

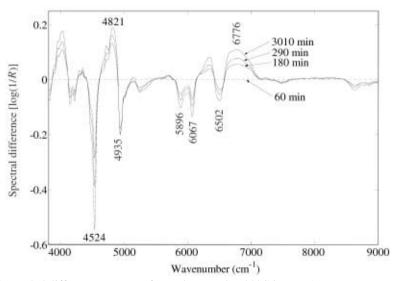Because of time limitations and experimental difficulties, only selected samples from Parts 1–3 were

Figure 3. SNV and detrended difference spectra of samples cured at 20°C in Part 1.

analysed for T_g and ΔH_r [Table 1(a) and (b)]. Details for the available samples for the PLSR calibrations are given in Table 3.

In each case, the matrix of spectra was transformed before calibration using MSC [Figure 2(b)] to improve the calibration results. Outliers were detected and removed during initial calibra-

tions: three for the T_g model and two for the mixing ratio model [marked in Tables 1(a) and 1(b)].

The regression coefficients for the models for T_g and ΔH_r are shown in Figure 5.

When comparing the most prominent peaks in Figure 5 with Figure 3 and Table 2, it can be seen, as expected, that a high value of ΔH_r and a low value of
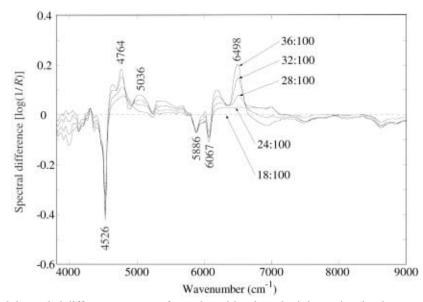

Figure 4. SNV and detrended difference spectra of samples with selected mixing ratios (hardener : resin) from Part 3.

Table 2. Assignments of bands in Figures 3 and 4.

	Epoxy group	Hydroxyl O–H	Primary amine
Figure 3 (cm^{-1})	4524 5896 6067	4821 6776	4935 6502
Figure 4 (cm^{-1})	4526 5886 6067	4764	5036 6498

Table 3. Statistics for the calibration samples.

	Samples	Minimum	Maximum	Mean	Std dev. s
T_g (°C)	31	41.5	98.8	75.6	14.2
ΔH_r (J g^{-1})	11	6.1	231.3	73.5	78.4
Hardener : resin	13	0.180	0.380	0.280	0.061

T_g are associated with a large number of epoxy and amine groups and a low number of hydroxyl groups. The root mean square error of cross-validation (*RMSECV*) was calculated using full cross-validadion ("leave one out").[42] Repeated random segmented cross-validation with ten segments was performed for the T_g model giving, on average, the same result as the full cross-validation. To evaluate the models, the ratio of the standard error of predic-tion to the standard deviation[44] was calculated according to *RPD* = s/*RMSECV* with the standard deviation s from Table 3 (except for the changes resulting from the removal of outliers). An *RPD*-value of 2.5 is considered acceptable, while a value of 10 is excellent. The mean of the standard deviations of the triplicate DSC analyses (s_{ref}) can be compared to the *RMSECV*. The results are given in Table 4.
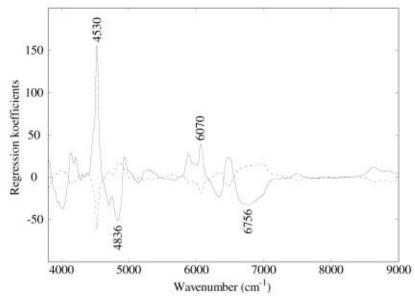

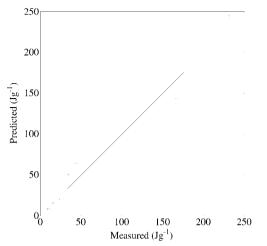Figure 5. Regression coefficients for the PLSR models for ΔH_r (solid line) and T_g (dotted line).

Table 4. Results for PLSR regressions using MSC and full cross-validation. s_{ref} is the mean of the standard deviations of the triplicate reference DSC analyses.
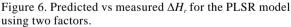
	Outliers	Factors	s_{ref}	*RMSECV*	*RPD*
T_g (°C)	3	3	1.5	7.2	1.9
ΔH_r (J g^{-1})	0	2	3.5	18	4.4
Hardener : resin	2	2		0.0040	16

Compared with the standard deviations of the triplicate determinations of ΔH_r and T_g, the *RMSECV*s are significantly higher, indicating that the NIR method is not as precise as the reference method. The values of *RPD*, however, indicate that the models for ΔH_r and mixing ratio are very good and fully applicable for the purpose of quality control and optimisation. The model for T_g is a little less than acceptable, but probably a calibration using more samples will show better performance.

In Figures 6–8, predicted vs measured values for the three models are plotted.

Conclusion

The present study has demonstrated that it is possible to replace the laborious and time-consuming DSC analyses of epoxy resins with NIR analysis,
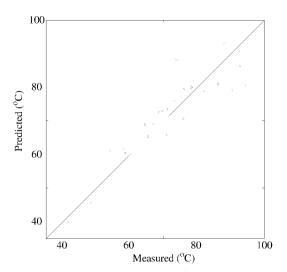
Figure 7. Predicted vs measured T_g for the PLSR model using three factors.

Figure 6. Predicted vs measured ΔH_r for the PLSR model using two factors.
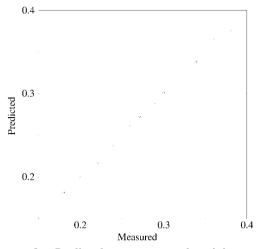
Figure 8. Predicted vs measured mixing ratio (hardner : resin) for the PLSR model using two factors.

and also that it is possible to predict the mixing ratio of hardener and resin. This can be used for quality control, for optimising the temperature program used in the curing process and for on-line control of the mixing ratio. The PLSR models showed good performance, with low to medium values of *RMSECV* compared with the standard deviation of the dependent variables. However, because of the relatively small set of samples, this is a preliminary study and the results should be confirmed by a larger experiment.

References

1. H. Dannenberg, *SPE Transactions*, January, 78 (1963).
2. N.A. St John and G.A. George, *Polymer* **33(13),** 2679 (1992).
3. B.-G. Min, Z.H. Stachurski, J.H. Hodgkin and G.R. Heath, *Polymer* **34(17),** 3620 (1993).
4. C.J. deBakker, G.A. George and N.A. St John, *Spectrochimica Acta Part A* **49(5/6),** 739 (1993).
5. C.J. deBakker, N.A. St John and G.A. George, *Polymer* **34(4),** 716 (1993).
6. B.-G. Min and Z.H. Stachurski, *Polymer* **34(17),** 3620 (1993).
7. K.E. Chike, M.L. Myrick, R.E. Lyon and S.M. Angel, *Appl. Spectrosc.* **47(10),** 1631 (1993).
8. K.A. Kozielski, G.A. George, N.A. St John and N.C. Billingham, *High Performance Polymers* **6,** 263 (1994).
9. V. Strehmel and T. Scherzer, *Eur. Polym. J.* **30(3),** 361 (1994).
10. L. Xu, J.H. Fu and J.R. Schlup, *J. Am. Chem. Soc.* **116**, 2821 (1994).
11. R.J. Varley, G. R. Heath, D.G. Hawthorne, J.H. Hodgkin and G.P. Simon, *Polymer* **36(7),** 1347 (1995).
12. J. Mijović and S. Andjelić, *Macromolecules* **28,** 2787 (1995).
13. S. Cossins, M. Connell, B. Cross, R. Winter and J. Kellar, *Appl. Spectrosc.* **50(7),** 900 (1996).
14. B. Ellis, M.S. Found and J.R. Bell, *J. Appl. Polym. Sci.* **59(10),** 1493 (1996).
15. G. Lachenal, A. Pierre and N. Poisson, *Micron* **27,** 329 (1996).
16. J. Mijović, S. Andjelić and J.M. Kenny, *Polym. Advan. Technol.* **7(1),** 1 (1996).
17. N. Poisson, G. Lachenal and H. Sautereau, *Vib. Spectrosc.* **12(2),** 237 (1996).
18. L. Xu and J.R. Schlup, *Appl. Spectrosc.* **50(1),** 109 (1996).
19. S. Paz-Abuin, A. Lopez-Quintela, M. Varela, M. Pazos-Pellin and P. Prendes, *Polymer* **38,** 3117 (1997).
20. B. Chabert, G. Lachenal and I. Stevenson, *Mikrochimica Acta* **Supl 13,** 321 (1997).
21. J.P. Dunkers, K.M. Flynn, M.T. Huang and W.G. McDonough, *Appl. Spectrosc.* **52(4),** 552 (1998).
22. G.R. Powell, P.A. Crosby, D.N. Waters, C.M. France, R.C. Spooncer and G.F. Fernando, *Smart Mater. Struct.* **7(4),** 557 (1998).
23. S. Andjelić and J. Mijović, *Macromolecules* **31(24),** 8463 (1998).
24. L. Xu and J.R. Schlup, *J. Appl. Polym. Sci.* **67,** 895 (1998).
25. A. López-Quintela, P. Prendes, M. Pazos-Pellín, M. Paz and S. Paz-Abuín, *Macromolecules* **31,** 4770 (1998).
26. D.G. Rogers, E. Marand, D.J.T. Hill and G.A. George, *High Performance Polymers* **11(1),** 27 (1999).
27. M. Fischer and C.D. Tran, *Anal. Chem.* **71(5),** 953 (1999).
28. P. Musto, E. Martuscelli, G. Ragosta, P. Russo and P. Villano, *J. Appl. Polym. Sci.* **74,** 532 (1999).
29. P. Musto, L. Mascia, G. Ragosta, G. Scarinzi and P. Villano, *Polymer* **41,** 565 (2000).
30. S.-J. Park, G.-H. Kwak, M. Sumita and J.-R. Lee, *Polym. Eng. Sci.* **40,** 2569 (2000).
31. J. Chen, T. Nakamura, K. Aoki, Y. Aoki and T. Utsunomiya, *J. Appl. Polym. Sci.* **79(2),** 214 (2001).
32. K. Dean, W.D. Cook, L. Rey, J. Galy and H. Sautereau, *Macromolecules* **34(19),** 6623 (2001).
33. P. Musto, E. Martuscelli, G. Ragosta and L. Mascia, *Polymer* **42(12),** 5189 (2001).
34. S.-J. Park, G.-H. Kwak, M.-K. Seo and J.-R. Lee, *J. Polym. Sci. Part B: Polym. Phys.* **39(3),** 326 (2001).
35. C. Billaud, M. Vandeuren, R. Legras and V. Carlier, *Appl. Spectrosc.* **56(11),** 1413 (2002).
36. C.E. Miller, *Appl. Spectrosc. Rev.* **26(4),** 277 (1991).

37. S.Y. Chang, N.S. Wang, *Multidimentional Spectroscopy of Polymers*, *ACS Symposium Series* **598,** 147 (1995).

38. G. Lachenal, *J. Near Infrared Spectrosc*. **6,** 299 (1998).

39. G. Höhne, W. Hemminger and H.-J. Flammersheim, *Differential Scanning Calorimetry.* Springer-Verlag (1996).

40. R.B. Prime, in *Thermal Characterization of Polymeric Materials* (2nd Edn), Ed by E.A. Turi. Academic Press, Ch. 6 (1997).

41. G. Wisanrakkit and J.K. Gillham, *J. Coatings Technol.* **62(783),** 35 (1990).

42. H. Martens and T. Næs, *Multivariate Calibration.* John Wiley & Sons, Chichester, UK (1991).

43. R.J. Barnes, M.S. Dhanoa and S.J. Lister, *Appl. Spectrosc.* **43(5),** 772 (1989).

44. P.C. Williams, in *Near-Infrared Technology in the Agricultural and Food Industries* (2nd Edn), Ed by P.C. Williams and K. Norris. American Association of Cereal Chemists, St Paul, MN, USA, Ch. 8 (2001).